C. R. Acad. Sci. Paris, Ser. I 355 (2017) 1298–1306

Contents lists available at ScienceDirect

C. R. Acad. Sci. Paris, Ser. I

www.sciencedirect.com

Numerical analysis

Semi-implicit staggered mesh scheme for the multi-layer shallow water system

Schéma semi-implicite sur maillages décalés pour le système shallow water *multi-couches*

Arnaud Duran [a], Jean-Paul Vila [b,c], Rémy Baraille [b,c,d]

[a] *Institut Camille-Jordan, Université Claude-Bernard, Lyon-1, France*
[b] *Institut de mathématiques de Toulouse, Université Paul-Sabatier, Toulouse-3, France*
[c] *INSA, Institut de mathématiques de Toulouse, Université Paul-Sabatier, Toulouse-3, France*
[d] *Service hydrographique et océanographique de la Marine, France*

ARTICLE INFO

Article history:
Received 13 June 2017
Accepted after revision 15 September 2017
Available online 26 November 2017

Presented by the Editorial Board

ABSTRACT

We present a semi-implicit scheme for a two-dimensional multilayer shallow water system with density stratification, formulated on general staggered meshes. The main result of the present note concerns the control of the mechanical energy at the discrete level, principally based on advective fluxes implying a diffusion term expressed in terms of the gradient pressure. The scheme is also designed to capture the dynamics of low-Froude-number regimes and offers interesting positivity and well-balancing results. A numerical test is proposed to highlight the scheme's efficiency in the one-layer case.

RÉSUMÉ

Nous proposons un schéma semi-implicite destiné à un modèle *shallow water* multicouches 2d avec stratification en densité, formulé sur maillages décalés généraux. Le principal résultat de cette note concerne le contrôle de l'énergie mécanique au niveau discret, qui se base principalement sur des flux advectifs faisant intervenir un terme de diffusion exprimé en fonction du gradient de pression. Le schéma est aussi conçu pour capturer les dynamiques des régimes à faible nombre de Froude et offre d'intéressantes propriétés en termes de positivité et préservation des états d'équilibre. Un test numérique est proposé pour illustrer l'efficacité du schéma dans le cas monocouche.

E-mail addresses: aduran@math.univ-toulouse.fr (A. Duran), vila@insa-toulouse.fr (J.-P. Vila), remy.baraille@shom.fr (R. Baraille).

https://doi.org/10.1016/j.crma.2017.09.011

1. Introduction

The present note introduces a staggered scheme designed to approximate the two-dimensional multilayer Shallow Water equations. This system is intended to account for the variations of the vertical density profile and correlated non-trivial pressure distribution, which characterize large scale oceanic flows. More precisely, the model considered here describes the dynamics of a superposition of N inviscid and immiscible layers with constant density, each of which being assumed to satisfy the hydrostatic pressure condition. Denoting $H_i(\mathbf{X},t)>0$ the effective mass (that is $\rho_i h_i$, where ρ_i is the density and h_i the layer thickness) and $\mathbf{u}_i(\mathbf{X},t)$ the horizontal velocity field attached to the *i-th* layer, function of the space and time variables $(\mathbf{X},t)$, the model is expressed as follows (see [14]):

$$\left\{\begin{array}{l}\partial_t H_i+\operatorname{div}(H_i\mathbf{u}_i)=0\,,\\ \partial_t(H_i\mathbf{u}_i)+\operatorname{div}(H_i\mathbf{u}_i\otimes\mathbf{u}_i)=-H_i\nabla\phi_i\,.\end{array}\right. \tag{1}$$

Note that this model applies to a large range of physical contexts, depending on the definition of the scalar potential ϕ_i and the number of layers N required to capture the flow dynamics. When the number of layers is greater than one, the pressure gradient $\nabla\phi_i$ involves a coupling between the layers, which is generally not conservative, which considerably complexifies the mathematical structure of the system. In the particular context of the multi-layer Shallow Water equations, and taking into account the topography z, we have:

$$\phi_i=g\left(z+\sum_{j=1}^{N}\frac{\rho_j}{\rho_{\max(i,j)}}h_j\right)\,, \tag{2}$$

g being the gravity constant. Thus, as soon as $N\geq 2$, we loose conservativity and the well-posedness of the problem must be subject to particular attention. The hyperbolicity is indeed closely linked to weak stratification contrast hypothesis and smallness assumptions on the velocity shear, as it is detailed in [10,3].

Returning to a more general point of view, the kinetic energy associated with the system (1) is defined by $\mathcal{K}_i=\frac{1}{2}H_i\,\|\mathbf{u}_i\|^2$ at the level of each layer i, and the potential energy is assumed to satisfy the relation

$$\partial_{H_i}\mathcal{E}=\phi_i\,. \tag{3}$$

Based on (2), this leads to the following potential energy:

$$\mathcal{E}=g\sum_{i=1}^{N}\left(\left(z+\frac{1}{2}\sum_{j=1}^{N}\frac{\rho_j h_j}{\rho_{\max(i,j)}}\right)\rho_i h_i\right)\,,$$

which generalizes the classical shallow water case. Of course, we should note that other physical systems may satisfy (3), as is the case for barotropic fluids for instance (see [11]). We also need to define $\mathbb{H}$ the Hessian of the potential energy, (*i.e.* the $N\times N$ matrix $\mathbb{H}_{i,j}=\partial_{H_iH_j}\mathcal{E}$), which can be expressed as a function of the mass vector $\mathbf{H}=(H_1,\cdots,H_N)$ and of the spatial position. In what follows, $\mathbb{H}$ will be supposed symmetric and positive-definite. Note that this condition is trivially satisfied in the present context, since it is clear from (2) that $\mathbb{H}$ is constant with respect to t and $\mathbf{X}$ (see [11,2]).

We recall here that for smooth solutions the total energy $E=\mathcal{E}+\sum_{i=1}^{N}\mathcal{K}_i$ satisfies the following conservation law:

$$\partial_t E+\sum_{i=1}^{N}\operatorname{div}\Big((H_i\phi_i+\mathcal{K}_i)\mathbf{u}_i\Big)=0\,. \tag{4}$$

In the following lines, we introduce a semi-implicit scheme on staggered grids for the model (1) and study its stability in the sense of numerical control of the total energy (*i.e.* we aim at obtaining a discrete equivalent of (4)). To address such an issue, and based on the formalism introduced in [4], followed later to treat the multilayer system in a collocated framework [11], the idea is to work on a regularized model, for which a shifted velocity is introduced in the mass and momentum equations:

$$\left\{\begin{array}{l}\partial_t H_i+\operatorname{div}\left(H_i(\mathbf{u}_i-\delta\mathbf{u}_i)\right)=0\,,\\ \partial_t(H_i\mathbf{u}_i)+\operatorname{div}\left(H_i\mathbf{u}_i\otimes(\mathbf{u}_i-\delta\mathbf{u}_i)\right)=-H_i\nabla\phi_i\,,\end{array}\right. \tag{5}$$

where $\delta\mathbf{u}_i$ stands for a generic perturbation. For regular solutions, it results a modified energy equation:

$$\partial_t E+\sum_{i=1}^{N}\operatorname{div}\Big((H_i\phi_i+\mathcal{K}_i)(\mathbf{u}_i-\delta\mathbf{u}_i)\Big)=-\sum_{i=1}^{N}\delta\mathbf{u}_i\cdot\nabla\phi_i\,. \tag{6}$$

Then, at least at the continuous level, we immediately see that a calibration of $\delta\mathbf{u}_i$ in terms of the pressure gradient (formally $\delta\mathbf{u}_i=\gamma\nabla\phi_i$ with $\gamma>0$) is expected to have regularizing virtues. We now seek for a discrete equivalent to this formal result.

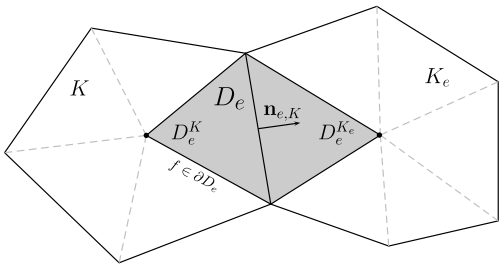

Fig. 1. Geometry associated with the Rannacher–Turek discretization.

2. Numerical scheme

We consider a partition $\mathcal{T}$ of the computational domain $\Omega \subset \mathbb{R}^2$ composed of $N_{\mathcal{T}}$ non-overlapping polygonal elements. The area of a generic cell K will be denoted by m_K and we denote by ∂K its boundary. For any edge e belonging to ∂K, we denote by K_e the corresponding adjacent cell and $\mathbf{n}_{e,K}$ the outward normal pointing to K_e (see Fig. 1). In what follows, m_e will stand for the length of the corresponding boundary interface. The concept of staggered discretizations is based on an evaluation of the velocity at locations that differs from the mass centers of the primal mesh, generally providing interesting stability properties. Historically, most of previsional platforms devoted to multiscale modelling make use of such environments. In the context of oceanic circulation, one can note HYCOM, ROMS [12] or NEMO [8,9] for instance. Many possibilities can be considered, such as the Rannacher–Turek (RT), Crouzeix–Raviart (CR) or Marker-And-Cell (MAC) discretizations, for instance. A general formalism attached to these discretizations has been developed and used within the implicit approaches [5,6] in the case of a one-layer system and in [7] for one- and two-phase pressure correction schemes, providing significant stability and consistency results. For the sake of clarity, we will illustrate the present approach in the frame of general RT grids, specifying that the forthcoming developments can easily be adapted to the other types of discretizations mentioned above. In this framework, the velocity unknowns are located at the faces of the primal mesh $\mathcal{T}$, standing for a representation of the average velocity computed over a dual mesh $\mathcal{T}^*$. At the level of an edge e, a dual element $D_e \in \mathcal{T}^*$ consists of a quadrilateral admitting e as diagonal and connecting the mass centers of the adjoining cells K and K_e, as illustrated in Fig. 1 in the case of a general polygonal grid. Let us finally introduce some useful notations. For a generic scalar function w, the notation $w^{\pm} = \frac{1}{2}(w \pm |w|)$ will refer to the positive and negative parts of w, and we set:

$$\overline{w}_e = \frac{1}{2}\left(w_{K_e} + w_K\right) \quad , \quad \boldsymbol{\delta} w_e = \frac{1}{2}\left(w_{K_e} - w_K\right)\mathbf{n}_{e,K}\,.$$

Similarly, for a vectorial piecewise function $\mathbf{w}$:

$$\overline{\mathbf{w}}_e = \frac{1}{2}\left(\mathbf{w}_{K_e} + \mathbf{w}_K\right) \quad , \quad \delta \mathbf{w}_e = \frac{1}{2}\left(\mathbf{w}_{K_e} - \mathbf{w}_K\right)\cdot\mathbf{n}_{e,K}\,.$$

Equipped with these notations, the numerical scheme we consider is the following:

$$\begin{cases} H_{K,i}^{n+1} & = H_{K,i}^n - \dfrac{\Delta t}{m_K}\displaystyle\sum_{e\in\partial K} \mathcal{F}_{e,i}^{n+1}\cdot\mathbf{n}_{e,K} m_e \\ H_{D_e,i}^{n+1}\mathbf{u}_{D_e,i}^{n+1} & = H_{D_e,i}^n \mathbf{u}_{D_e,i}^n - \dfrac{\Delta t}{m_{D^e}}\displaystyle\sum_{f\in\partial D_e}\left(\mathbf{u}_{D_e,i}^n\left(\mathcal{F}_{f,i}^{n+1}\cdot\mathbf{n}_{f,D_e}\right)^+ + \mathbf{u}_{D_e^f,i}^n\left(\mathcal{F}_{f,i}^{n+1}\cdot\mathbf{n}_{f,D_e}\right)^-\right)m_f - \Delta t H_{D_e,i}^{n+1}(\nabla\boldsymbol{\Phi})_{e,i}\,. \end{cases} \tag{7}$$

In the expression above, D_e^f refers to the dual cell sharing the edge f with D_e, and we use m_{D_e} and m_f to design the cell areas and edge lengths of the corresponding dual elements, following the notations of the primal mesh. The formula for the pressure gradient is directly deduced from the discrete grad/div duality with respect to the L^2 inner product (see also [6]):

$$(\nabla\boldsymbol{\Phi})_{e,i} = \frac{m_e}{m_{D_e}}\left(\Phi_{K_e,i}^{n+1} - \Phi_{K,i}^{n+1}\right)\mathbf{n}_{e,K} = 2\frac{m_e}{m_{D_e}}\delta\Phi_{e,i}^{n+1}\,. \tag{8}$$

The auxiliary water height $H_{D_e,i}^{n+1}$ is defined as a weighted average implying the adjoining cells of the primal mesh:

$$m_{D_e} H_{D_e,i}^{n+1} = m_{D_e^K} H_{K,i}^{n+1} + m_{D_e^{K_e}} H_{K_e,i}^{n+1}\,, \tag{9}$$

and we suppose that the evolution of this quantity is governed by the following scheme:

$$H_{D_e,i}^{n+1} - H_{D_e,i}^n = -\frac{\Delta t}{m_{D^e}}\sum_{f\in\partial D_e}\mathcal{F}_{f,i}^{n+1}\cdot\mathbf{n}_{f,D_e} m_f\,. \tag{10}$$

This discrete conservation equation is fundamental to attach an energy budget to the numerical system. The numerical fluxes $\mathcal{F}_{f,i}^{n+1}$ are actually expressed in terms of combinations of the original fluxes $\mathcal{F}_{e,i}^{n+1}$, with varying coefficients depending on the mesh discretization. These construction aspects can be found in [1]. We now define the numerical fluxes:

$$\mathcal{F}_{e,i}^{n+1} = H_{D_e,i}^{n+1}\mathbf{u}_{D_e,i}^{n} - \Pi_{e,i}^{n+1}\,, \tag{11}$$

where

$$\Pi_{e,i}^{n+1} = 2\gamma\,\Delta t\frac{m_e}{m_{D_e}}H_{D_e,i}^{n+1}\delta\Phi_{e,i}^{n+1}\,,\quad \gamma \geq 1\,, \tag{12}$$

is a stabilization term designed to ensure a discrete energy control. Note that this term is somehow expressed in terms of numerical gradient pressure (through $\delta\Phi_{e,i}^{n+1}$), which stands for a discrete equivalent of $\delta\mathbf{u}_i$ introduced at the continuous level to control the energy budget (see (6) and discussion below). For future developments, we lastly need the time evolution of the velocity, which is derived from the momentum equations using (10):

$$\mathbf{u}_{D_e,i}^{n+1} = \mathbf{u}_{D_e,i}^{n} - \frac{\Delta t}{m_{D^e}}\sum_{f\in\partial D_e}\frac{\mathbf{u}_{D_e^f,i}^{n} - \mathbf{u}_{D_e,i}^{n}}{H_{D_e,i}^{n+1}}\big(\mathcal{F}_{f,i}^{n+1}\cdot\mathbf{n}_{f,D_e}\big)^{-}m_f - \Delta t(\nabla\boldsymbol{\Phi})_{e,i}\,. \tag{13}$$

3. Main result: control of the mechanical energy

The following section is intended to show that the present approach prevents from non-physical production of mechanical energy. More precisely, defining $\mathcal{E}_K^n$ and $\mathcal{K}_{D_e,i}^n = \frac{1}{2}H_{D_e,i}^n\|\mathbf{u}_{D_e,i}^n\|^2$ the local potential and kinetic energies, available at the primal and dual meshes respectively, the discrete total energy corresponds to:

$$E^n = \sum_{K\in\mathcal{T}} m_K\mathcal{E}_K^n + \sum_{D_e\in\mathcal{T}^*} m_{D_e}\Big(\sum_{i=1}^{N}\mathcal{K}_{D_e,i}^n\Big)\,, \tag{14}$$

and we have the following result.

Theorem 3.1. *We consider the scheme (7), together with the numerical fluxes (11), (12), and the discrete gradient pressure (8). Suppose that the time step satisfies the following CFL condition:*

$$\frac{\Delta t}{m_{D^e}}\sum_{f\in\partial D_e} -\big(\mathcal{F}_{f,i}^{n+1}\cdot\mathbf{n}_{f,D_e}\big)^{-}m_f < \frac{1}{2}H_{D_e,i}^{n+1}\,. \tag{15}$$

We have:

$$E^{n+1} - E^n \leq 0\,.$$

The proof is organized around the following steps:

(A) estimation of the kinetic energy production (Lemma 3.1);
(B) estimation of the potential energy production (Lemma 3.2);
(C) control of the total energy: we gather the two inequalities resulting from #*A* and #*B* to deduce the sufficient condition $\gamma \geq 1$ in the advective fluxes (12) (proof of Theorem 3.1).

Lemma 3.1. *Estimation of the kinetic energy production. We have the following inequality:*

$$\mathcal{K}_{D_e,i}^{n+1} - \mathcal{K}_{D_e,i}^{n} + \frac{\Delta t}{m_{D^e}}\sum_{f\in\partial D_e}\big(\mathcal{G}_{\mathcal{K},f,i}^{n+1}\cdot\mathbf{n}_{f,D_e}\big)m_f \leq \mathcal{R}_{\mathcal{K},e,i} - \mathcal{Q}_{\mathcal{K},e,i}\,, \tag{16}$$

with

$$\mathcal{G}_{\mathcal{K},f,i}^{n+1}\cdot\mathbf{n}_{f,D_e} = \frac{1}{2}\|\mathbf{u}_{D_e,i}^{n}\|^2\big(\mathcal{F}_{f,i}^{n+1}\cdot\mathbf{n}_{f,D_e}\big)^{+} + \frac{1}{2}\left\|\mathbf{u}_{D_e^f,i}^{n}\right\|^2\big(\mathcal{F}_{f,i}^{n+1}\cdot\mathbf{n}_{f,D_e}\big)^{-}\,,$$
$$\mathcal{Q}_{\mathcal{K},e,i} = \Delta t\, H_{D_e,i}^{n+1}\mathbf{u}_{D_e,i}^{n}\cdot(\nabla\boldsymbol{\Phi})_{e,i}\,,$$
$$\mathcal{R}_{\mathcal{K},e,i} = (\Delta t)^2 H_{D_e,i}^{n+1}\left\|(\nabla\boldsymbol{\Phi})_{e,i}\right\|^2\,.$$

Proof. Using the equation on the velocity (13), we have:

$$H^{n+1}_{D_e,i}(\mathbf{u}^{n+1}_{D_e,i}-\mathbf{u}^{n}_{D_e,i})\cdot\mathbf{u}^{n}_{D_e,i}=-\frac{\Delta t}{m_{D^e}}\sum_{f\in\partial D_e}(\mathbf{u}^{n}_{D^f_e,i}-\mathbf{u}^{n}_{D_e,i})\cdot\mathbf{u}^{n}_{D_e,i}\big(\mathcal{F}^{n+1}_{f,i}\cdot\mathbf{n}_{f,D_e}\big)^{-}m_f-\Delta t H^{n+1}_{D_e,i}(\nabla\mathbf{\Phi})_{e,i}\cdot\mathbf{u}^{n}_{D_e,i}\,.$$

We then use the relation $(\mathbf{a}-\mathbf{b})\cdot\mathbf{b}=\frac{1}{2}\|\mathbf{a}\|^2-\frac{1}{2}\|\mathbf{b}\|^2-\frac{1}{2}\|\mathbf{a}-\mathbf{b}\|^2$, to write:

$$\begin{aligned}&H^{n+1}_{D_e,i}\Big(\frac{1}{2}\Big\|\mathbf{u}^{n+1}_{D_e,i}\Big\|^2-\frac{1}{2}\Big\|\mathbf{u}^{n}_{D_e,i}\Big\|^2-\frac{1}{2}\Big\|\mathbf{u}^{n+1}_{D_e,i}-\mathbf{u}^{n}_{D_e,i}\Big\|^2\Big)\\&\quad=-\frac{\Delta t}{m_{D^e}}\sum_{f\in\partial D_e}\Big(\frac{1}{2}\Big\|\mathbf{u}^{n}_{D^f_e,i}\Big\|^2-\frac{1}{2}\Big\|\mathbf{u}^{n}_{D_e,i}\Big\|^2-\frac{1}{2}\Big\|\mathbf{u}^{n}_{D^f_e,i}-\mathbf{u}^{n}_{D_e,i}\Big\|^2\Big)\big(\mathcal{F}^{n+1}_{f,i}\cdot\mathbf{n}_{f,D_e}\big)^{-}m_f-\Delta t H^{n+1}_{D_e,i}(\nabla\mathbf{\Phi})_{e,i}\cdot\mathbf{u}^{n}_{D_e,i}\,.\end{aligned}$$

Reorganizing this expression, and using the auxiliary mass equation (10), the previous equality becomes:

$$\begin{aligned}\mathcal{K}^{n+1}_{D_e,i}-\mathcal{K}^{n}_{D_e,i}=&-\frac{\Delta t}{m_{D^e}}\sum_{f\in\partial D_e}\Big(\frac{1}{2}\Big\|\mathbf{u}^{n}_{D_e,i}\Big\|^2\big(\mathcal{F}^{n+1}_{f,i}\cdot\mathbf{n}_{f,D_e}\big)^{+}+\frac{1}{2}\Big\|\mathbf{u}^{n}_{D^f_e,i}\Big\|^2\big(\mathcal{F}^{n+1}_{f,i}\cdot\mathbf{n}_{f,D_e}\big)^{-}\Big)m_f\\&+\frac{1}{2}H^{n+1}_{D_e,i}\Big\|\mathbf{u}^{n+1}_{D_e,i}-\mathbf{u}^{n}_{D_e,i}\Big\|^2+\frac{\Delta t}{m_{D^e}}\sum_{f\in\partial D_e}\frac{1}{2}\Big\|\mathbf{u}^{n}_{D^f_e,i}-\mathbf{u}^{n}_{D_e,i}\Big\|^2\big(\mathcal{F}^{n+1}_{f,i}\cdot\mathbf{n}_{f,D_e}\big)^{-}m_f\\&-\Delta t H^{n+1}_{D_e,i}(\nabla\mathbf{\Phi})_{e,i}\cdot\mathbf{u}^{n}_{D_e,i}\,.\end{aligned}\tag{17}$$

We then set:

$$S_{e,i}=\frac{1}{2}H^{n+1}_{D_e,i}\Big\|\mathbf{u}^{n+1}_{D_e,i}-\mathbf{u}^{n}_{D_e,i}\Big\|^2+\frac{\Delta t}{m_{D^e}}\sum_{f\in\partial D_e}\frac{1}{2}\Big\|\mathbf{u}^{n}_{D^f_e,i}-\mathbf{u}^{n}_{D_e,i}\Big\|^2\big(\mathcal{F}^{n+1}_{f,i}\cdot\mathbf{n}_{f,D_e}\big)^{-}m_f\,.$$

An upper bound can be deduced for the first term of $S_{e,i}$ with the use of Jensen's inequality:

$$\frac{1}{2}H^{n+1}_{D_e,i}\Big\|\mathbf{u}^{n+1}_{D_e,i}-\mathbf{u}^{n}_{D_e,i}\Big\|^2\le H^{n+1}_{D_e,i}(\Delta t)^2\big\|(\nabla\mathbf{\Phi})_{e,i}\big\|^2+\frac{1}{H^{n+1}_{D_e,i}}\Big(\frac{\Delta t}{m_{D^e}}\Big)^2\Big\|\sum_{f\in\partial D_e}(\mathbf{u}^{n}_{D^f_e,i}-\mathbf{u}^{n}_{D_e,i})\big(\mathcal{F}^{n+1}_{f,i}\cdot\mathbf{n}_{f,D_e}\big)^{-}m_f\Big\|^2\,.$$

Then, invoking the Cauchy–Schwarz inequality, we have:

$$\begin{aligned}&\Big\|\sum_{f\in\partial D_e}(\mathbf{u}^{n}_{D^f_e,i}-\mathbf{u}^{n}_{D_e,i})\big(\mathcal{F}^{n+1}_{f,i}\cdot\mathbf{n}_{f,D_e}\big)^{-}m_f\Big\|^2=\\&\qquad\le\Big(\sum_{f\in\partial D_e}\Big\|\mathbf{u}^{n}_{D^f_e,i}-\mathbf{u}^{n}_{D_e,i}\Big\|^2\big(\mathcal{F}^{n+1}_{f,i}\cdot\mathbf{n}_{f,D_e}\big)^{-}m_f\Big)\Big(\sum_{f\in\partial D_e}\big(\mathcal{F}^{n+1}_{f,i}\cdot\mathbf{n}_{f,D_e}\big)^{-}m_f\Big)\end{aligned}$$

Thus:

$$\begin{aligned}S_{e,i}\le&H^{n+1}_{D_e,i}(\Delta t)^2\big\|(\nabla\mathbf{\Phi})_{e,i}\big\|^2+\frac{\Delta t}{m_{D^e}}\sum_{f\in\partial D_e}\Big\|\mathbf{u}^{n}_{D^f_e,i}-\mathbf{u}^{n}_{D_e,i}\Big\|^2\big(\mathcal{F}^{n+1}_{f,i}\cdot\mathbf{n}_{f,D_e}\big)^{-}m_f\\&\times\Big[1/2-\frac{\Delta t}{m_{D^e}}\sum_{f\in\partial D_e}\frac{-\big(\mathcal{F}^{n+1}_{f,i}\cdot\mathbf{n}_{f,D_e}\big)^{-}}{H^{n+1}_{D_e,i}}m_f\Big]\end{aligned}$$

The second term being assumed negative according to the CFL condition (15), on gets the announced result injecting the resulting estimation of $S_{e,i}$ into (17). □

Remark 3.1. By reason of the semi-implicit formalism, the time step restriction (15) can actually be seen as a classical CFL governed by the inertial forces only, subject to an $\mathcal{O}(\Delta t)$ perturbation. More precisely, one can establish a sufficient condition for (15) implying the collocated fluxes only, of the form:

$$\frac{\Delta t}{m_K}\sum_{e\in\partial K}|\mathcal{F}^{n+1}_{e,i}\cdot\mathbf{n}_{e,K}|m_f<\beta H^{n}_{K,i}\,,\tag{18}$$

where β is a constant verifying $0 < \beta \leq 1$, to be calibrated depending on the choice of the staggered discretization. Then, after basic computations, one gets that (18) is indeed ensured under a time step satisfying the local condition:

$$\Delta t \max\left(\frac{m_{\partial K}}{m_K}, \frac{m_{\partial K_e}}{m_{K_e}}\right)\left(|\mathbf{u}^n_{D_e,i}\cdot\mathbf{n}_{e,K}| + 2\gamma\,\Delta t\frac{m_e}{m_{D_e}}|\delta\Phi^{n+1}_{e,i}\cdot\mathbf{n}_{e,K}|\right) < \left(\frac{\beta}{1+\beta}\right)\frac{\min(H^{n+1}_{K,i}, H^{n+1}_{K_e,i})}{H^{n+1}_{D_e,i}}\,.$$

Lemma 3.2. *Estimation of the potential energy production. We have the following inequality:*

$$\mathcal{E}^{n+1}_K - \mathcal{E}^n_K + \frac{\Delta t}{m_K}\sum_{e\in\partial K}\sum_{i=1}^{N}(\mathcal{G}^{n+1}_{\mathcal{E},e,i}\cdot\mathbf{n}_{e,K})m_e \leq \mathcal{Q}_{\mathcal{E},K} - \mathcal{R}_{\mathcal{E},K}\,, \tag{19}$$

with

$$\mathcal{G}^{n+1}_{\mathcal{E},e,i}\cdot\mathbf{n}_{e,K} = \overline{\Phi}^{n+1}_{e,i}\,\mathcal{F}^{n+1}_{e,i}\cdot\mathbf{n}_{e,K}\,,$$

$$\mathcal{Q}_{\mathcal{E},K} = \frac{\Delta t}{m_K}\sum_{e\in\partial K}\sum_{i=1}^{N} H^{n+1}_{D_e,i}\mathbf{u}^n_{D_e,i}\cdot\delta\Phi^{n+1}_{e,i}m_e\,,$$

$$\mathcal{R}_{\mathcal{E},K} = \frac{\Delta t}{m_K}\sum_{e\in\partial K}\sum_{i=1}^{N}\Pi^{n+1}_{e,i}\cdot\delta\Phi^{n+1}_{e,i}m_e\,.$$

Proof. Denoting $\mathbf{X}_K$ the mass center of the cell K and $\mathbf{H}^n_K$ the corresponding mass vector at time n, Taylor's formula gives, for a certain $0 \leq s_K \leq 1$:

$$\mathcal{E}^{n+1}_K - \mathcal{E}^n_K = \sum_{i=1}^{N}(H^{n+1}_{K,i} - H^n_{K,i})\Phi^{n+1}_{K,i} - \frac{1}{2}\sum_{i=1}^{N}\sum_{j=1}^{N}(H^{n+1}_{K,i} - H^n_{K,i})\mathbb{H}^{n+s_K}_{i,j,K}(H^{n+1}_{K,j} - H^n_{K,j})\,,$$

where $\mathbb{H}^{n+s_K}_{i,j,K} = \mathbb{H}_{i,j}\left(s_K\mathbf{H}^{n+1}_K + (1-s_K)\mathbf{H}^n_K, \mathbf{X}_K\right)$. The Hessian of the system being definite positive, the second term of the right-hand side is negative, and we have:

$$\mathcal{E}^{n+1}_K - \mathcal{E}^n_K \leq -\frac{\Delta t}{m_K}\sum_{e\in\partial K}\sum_{i=1}^{N}\Phi^{n+1}_{K,i}\mathcal{F}^{n+1}_{e,i}\cdot\mathbf{n}_{e,K}m_e\,.$$

We then proceed to the following decomposition:

$$\Phi^{n+1}_{K,i}\mathcal{F}^{n+1}_{e,i}\cdot\mathbf{n}_{e,K} = \mathcal{G}^{n+1}_{\mathcal{E},e,i}\cdot\mathbf{n}_{e,K} - H^{n+1}_{D_e,i}\mathbf{u}^n_{D_e,i}\cdot\delta\Phi^{n+1}_{e,i} + \Pi^{n+1}_{e,i}\cdot\delta\Phi^{n+1}_{e,i}\,,$$

to fall on the desired contributions. □

We can now establish the result stated in Theorem 3.1.

Proof of Theorem 3.1.

Terms in $\mathcal{Q}$:

Summing the kinetic and potential contributions over the dual and original mesh respectively, we obtain the two following terms:

$$-\sum_{D_e\in\mathcal{T}^*} m_{D_e}\sum_{i=1}^{N}\mathcal{Q}_{\mathcal{K},e,i} = -\Delta t\sum_{D_e\in\mathcal{T}^*}\sum_{i=1}^{N} m_{D_e}H^{n+1}_{D_e,i}\mathbf{u}^n_{D_e,i}\cdot(\nabla\boldsymbol{\Phi})_{e,i}\,.$$

$$\sum_{K\in\mathcal{T}} m_K\mathcal{Q}_{\mathcal{E},K} = \Delta t\sum_{K\in\mathcal{T}}\sum_{e\in\partial K}\sum_{i=1}^{N} H^{n+1}_{D_e,i}\mathbf{u}^n_{D_e,i}\cdot\delta\Phi^{n+1}_{e,i}m_e\,.$$

For a given layer i and a dual element D_e, we are consequently in the presence of three contributions:

- one from the kinetic part:

$$-\Delta t m_{D_e}H^{n+1}_{D_e,i}\mathbf{u}^n_{D_e,i}\cdot(\nabla\boldsymbol{\Phi})_{e,i}\,;$$

- two identical terms from the potential part, coming from each side of the interface e:

$$2\Delta t m_e H^{n+1}_{D_e,i}\mathbf{u}^n_{D_e,i}\cdot\delta\Phi^{n+1}_{e,i} = \Delta t\, m_e\, H^{n+1}_{D_e,i}\mathbf{u}^n_{D_e,i}\cdot\left(\Phi^{n+1}_{K_e,i}-\Phi^{n+1}_{K,i}\right)\mathbf{n}_{e,K}\,.$$

From this, it is straightforward to verify that the discrete pressure gradient (8) provides an exact balance of these terms.

Terms in $\mathcal{R}$:

We focus now on the terms $\mathcal{R}_{\mathcal{E},K}$ and $\mathcal{R}_{\mathcal{K},e,i}$. The resulting contributions are respectively:

$$-\sum_{K\in\mathcal{T}} m_K\mathcal{R}_{\mathcal{E},K} = -\Delta t\sum_{K\in\mathcal{T}}\sum_{e\in\partial K}\sum_{i=1}^{N}\Pi^{n+1}_{e,i}\cdot\delta\Phi^{n+1}_{e,i}m_e\,.$$

$$\sum_{D_e\in\mathcal{T}^*} m_{D_e}\sum_{i=1}^{N}\mathcal{R}_{\mathcal{K},e,i} = \sum_{D_e\in\mathcal{T}^*}\sum_{i=1}^{N} m_{D_e}H^{n+1}_{D_e,i}(\Delta t)^2\|(\nabla\boldsymbol{\Phi})_{e,i}\|^2\,.$$

Again, for a given layer i and dual element D_e, we have three contributions:

- one from the kinetic part:

$$m_{D_e}H^{n+1}_{D_e,i}(\Delta t)^2\|(\nabla\boldsymbol{\Phi})_{e,i}\|^2\,; \tag{20}$$

- two from the potential, giving:

$$-2\Delta t m_e\Pi^{n+1}_{e,i}\cdot\delta\Phi^{n+1}_{e,i}\,.$$

Using (12) and (8), we have:

$$2\Delta t m_e\,\Pi^{n+1}_{e,i}\cdot\delta\Phi^{n+1}_{e,i} = (\Delta t)^2 m_{D_e}H^{n+1}_{D_e,i}\gamma\,\left\|(\nabla\boldsymbol{\Phi})_{e,i}\right\|^2\,. \tag{21}$$

Gathering (20) and (21), we finally obtain that the energy control is ensured under the condition $\gamma\geq 1$. □

Remark 3.2. Naturally, a more general result consists in keeping the previous right-hand side in the energy budget, with the possibility of introducing numerical dissipation for $\gamma > 1$.

$$E^{n+1}-E^n \leq (\Delta t)^2 H^{n+1}_{D_e,i}m_{D_e}\|(\nabla\boldsymbol{\Phi})_{e,i}\|^2(1-\gamma)\,.$$

4. Additional properties

In addition of mechanical energy dissipation and positivity results, the present scheme enjoys other fundamental stability properties, which are the preservation of motionless steady states and the consistency with the asymptotics observed in low-Froude-number regimes. Regarding the preservation of the equilibrium states at rest, defined by $\mathbf{u}^n_{K,i}=0$, $\Phi^n_{K,i}=\tilde{\Phi}_i$ for all $K\in\mathcal{T}$, on obtains $h^{n+1}_{K,i}=h^n_{K,i}$ as the unique solution of the mass equation, and hence $\Phi^{n+1}_{K,i}=0$. Using (8) and (11), this immediately gives the preservation of the initial rest state. The asymptotic preserving features can be established with the support of an analysis at the continuous level in space, as done in [2].

5. Numerical experiments

The following section presents some numerical results based on the Thacker's solutions [13] in the one layer case. There are not many available solutions for the non-linear shallow water equations involving complex configurations, including non-trivial topographies and moving boundaries. In this respect, the present class of benchmarks is frequently used in the validation steps of operational codes. The present simulation involves a periodic flow evolving over a parabolic bathymetry:

$$z(x,y) = D_0\left(\frac{x^2}{L^2}+\frac{y^2}{L^2}\right),$$

for which the following analytical solution is:

$$\begin{aligned}\zeta(x,y,t) &= 2\eta D_0\left(\frac{x}{L}\cos(\omega t)-\frac{y}{L}\sin(\omega t)-\frac{2\eta}{L}\right)\\ u(x,y,t) &= -\eta\omega\sin(\omega t)\\ v(x,y,t) &= -\eta\omega\cos(\omega t)\end{aligned},$$

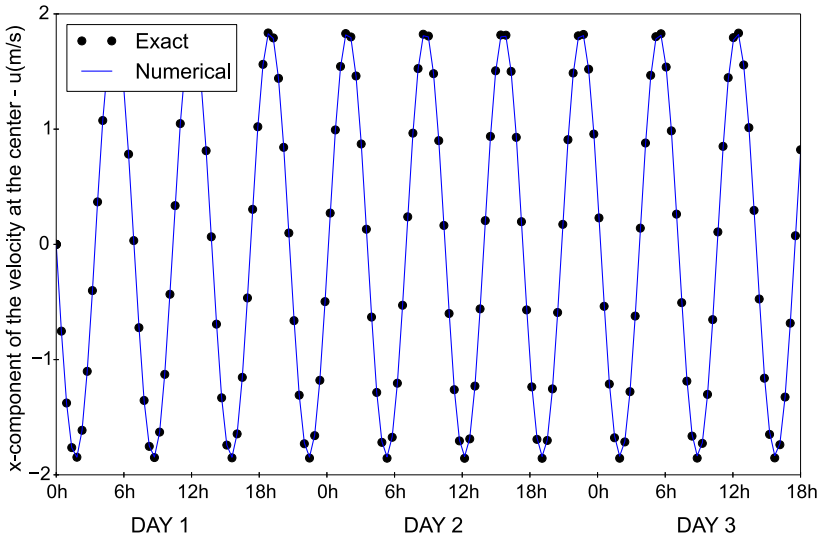

Fig. 2. Periodic evolution of the x-component of the velocity, computed at the center of the basin. Exact vs. numerical.

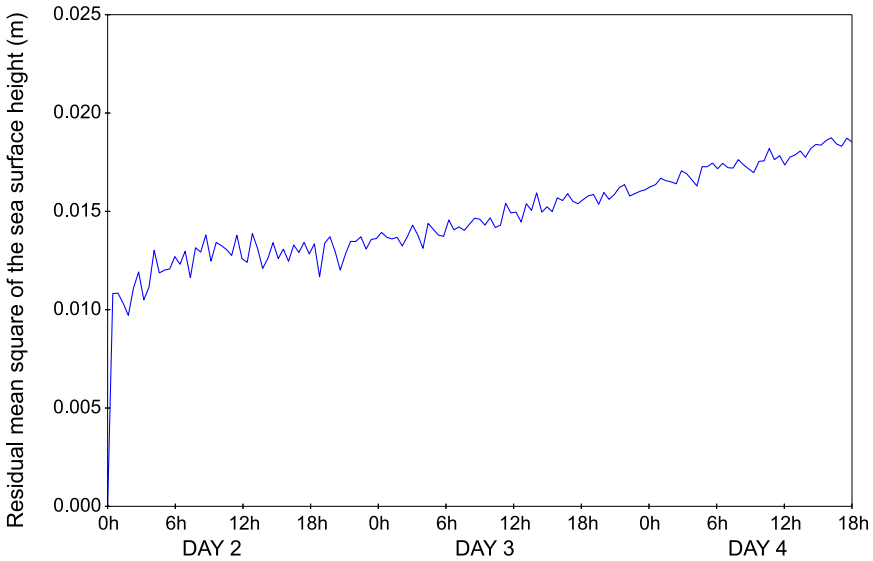

Fig. 3. Evolution of the sea surface height RMS error.

ζ standing for the free surface elevation with respect to the maximal depth D_0. The frequency is given by $\omega = f/2 + \sqrt{f^2/4 + 2gD_0/L^2}$, f being the Coriolis parameter. Following the COMODO experiment, f is set to 10^{-4} s^{-1} and $D_0 = 10$ m. The constant L corresponding to the basin width at rest is 80 km and the adimensional amplitude η is set to 0.1. Friction effects are neglected during the simulation. Computations are run on a 201×201 square grid with a space step of 1 km. The time step and gamma have been set respectively to 60 s and 1. The integration time is fixed to 3 days.

We can observe in Fig. 2 the time evolution of the horizontal component of the velocity, computed at the center of the basin. We obtain a very good matching with the analytical solution, highlighting a negligible rate of numerical dissipation throughout the simulation. A numerical error quantification is proposed in Fig. 3, with the Residual Mean Square deviation (RMS) of the sea surface height, formally computed from:

$$\left[\frac{1}{N_w}\sum_{n=0}^{N_t}\left(\zeta_{num}^n - \zeta_{th}^n\right)^2\right]^{1/2},$$

N_w being the theoretical number of wet points and N_t the number of time steps. We can observe a very moderate evolution of the RMS error with time, which is less than 2 cm at the end of the simulation, while it reaches around 4 cm in the original COMODO benchmark with HYCOM and the same set of initialization parameters.

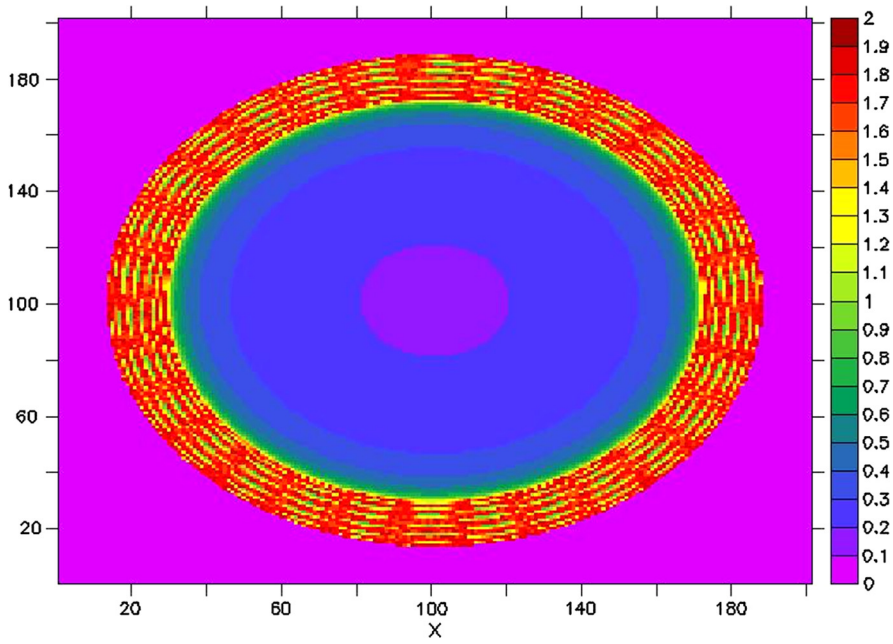

Fig. 4. Representation of the maximum of the Froude number in the computational domain, computed over 11 periods.

To complete the picture, Fig. 4 shows the distribution of the maximum Froude number value throughout the computational domain, computed over 11 periods. Starting from zero at the center, the Froude number tends to increase as we reach the moving boundary, inducing a rough regime change close to the wet/dry interface. As it has been already observed in the collocated framework (see [2]), the present approach is particularly well-suited to capture this quite complex dynamics, which explains the slight improvements with respect to the classical approaches, notably in a long time behaviour.

Additionally, in the presence of very low-Froude-number regimes, the preliminary results are in conformity with those obtained in the collocated context [2], in which we highlighted the considerable benefits when compared with some classical solvers, while remaining consistent with the discrete entropy inequality.

References

[1] G. Ansanay-Alex, F. Babik, J.-C. Latché, D. Vola, An L2 stable approximation of the Navier Stokes convection operator for low-order non-conforming finite elements, Int. J. Numer. Methods Fluids 66 (5) (2011) 555–580.
[2] F. Couderc, A. Duran, J.-P. Vila, An explicit asymptotic preserving low-Froude scheme for the multilayer shallow water model with density stratification, J. Comput. Phys. 343 (2017) 235–270.
[3] V. Duchene, The multilayer shallow water system in the limit of small density contrast, Asymptot. Anal. 98 (3) (2016) 189–235.
[4] N. Grenier, J.-P. Vila, P. Villedieu, An accurate low-Mach scheme for a compressible two-fluid model applied to free-surface flows, J. Comput. Phys. 252 (2013) 1–19.
[5] R. Herbin, J.-C. Latché, T. Nguyen, Explicit staggered schemes for the compressible Euler equations, ESAIM Proc. 40 (2014) 83–102.
[6] R. Herbin, W. Kheriji, J.-C. Latché, On some implicit and semi-implicit staggered schemes for the shallow water and Euler equations, ESAIM: Math. Model. Numer. Anal. 48 (6) (2014) 1807–1857.
[7] W. Kheriji, R. Herbin, J.-C. Latché, Pressure correction staggered schemes for barotropic one-phase and two-phase flows, Comput. Fluids 88 (2013) 524–542.
[8] M. Leclair, G. Madec, A conservative leapfrog time stepping method, Ocean Model. 30 (2–3) (2009) 88–94.
[9] G. Madec, NEMO Reference Manual, Ocean Dynamics Component: NEMO OPA. Preliminary Version, Technical Report 27, Institut Pierre–Simon–Laplace, 2008, pp. 3723–3750.
[10] R. Monjarret, The Multi-Layer Shallow Water Model with Free Surface. Numerical Treatment of the Open Boundaries, PHD, Institut national polytechnique de Toulouse, Université de Toulouse, 2014.
[11] M. Parisot, J.-P. Vila, Centered-potential regularization of advection upstream splitting method: application to the multilayer shallow water model in the low-Froude-number regime, SIAM J. Numer. Anal. 54 (5) (2016) 3083–3104.
[12] A.F. Shchepetkin, J.C. McWilliams, The regional oceanic modeling system (ROMS): a split-explicit, free-surface, topography-following-coordinate oceanic model, Ocean Model. 9 (2005) 347–404.
[13] W.C. Thacker, Some exact solutions to the nonlinear shallow water wave equations, J. Fluid Mech. 107 (1981) 499–508.
[14] G.K. Vallis, Atmospheric and Oceanic Fluid Dynamics, Cambridge University Press, Cambridge, UK, 2006.